14th European Signal Processing Conference (EUSIPCO 2006), Florence, Italy, September 4-8, 2006, copyright by EURASIP

# A WAVELET DOMAIN FILTER FOR CORRELATED SPECKLE

*Stian Solbø† and Torbjørn Eltoft‡*

† Norut IT, Tromsø, Norway. Tel: +47 776 29 425, e-mail: stian.solboe@itek,norut,no
‡ Institute of Physics, University of Tromsø, Tromsø, Norway. E-mail: torbjorn.eltoft@phys.uit.no

## ABSTRACT

In this paper we assume that both the radar cross section and the speckle noise in SAR images are spatially correlated. We develop a wavelet domain linear minimum mean square error filter to remove the speckle noise. The autocorrelation functions in the wavelet domain are estimated from the single look complex SAR image. Preliminary studies show that proposed filter introduces less bias compared to performed the filtering in the image domain, but does not achieve the same level of smoothing. The proposed filter does not depend on sliding windows to avoid boundary effects.

## 1. INTRODUCTION

Speckle is a phenomenom inherent in coherent imaging systems with spatial resolution greater than the wavelength. Synthetic aperture radar (SAR) is an example of such an imaging system. Due to the roughness of the imaged surface, each resolution cell will contain several scatterers, and the resulting image will have a granular appearance due to constructive and destructive interference. Speckle appears as *spatially correlated*, *multiplicative noise* that is statistically independent of the image intensity, although it is a radiometric feature of the imaged object. The granular nature of speckled images makes them hard to interpret, both for the human eye and automated segmentation and classification algorithms.

Over the years, speckle noise has been widely studied, and several methods have been developed to reduce the speckle noise, and hence increase the usability of speckled images in e.g. classification. The simplest method is multilooking, or *incoherent averaging*, which increase the SNR at the cost of reduced spatial resolution. Filters that assume statistical models for the speckle and use maximum a posteriori (MAP) filtering, like the Gamma-MAP filter [1], are quite common for *despeckling*. Other filters are based on spectral models for the speckle statistics and use local linear minimum square error (LLMMSE) filtering to remedy the speckling effect [2].

During the last decade, many speckle filters utilizing the wavelet transform (WT) [3] have been proposed by several authors. The WT has many feasible properties, like possibility to multi-scale filtering, which makes it well suited for noise reduction in a number of applications. Further, the WT is a sparse transform, compressing the signal energy to a small number of wavelet coefficients and leaving the majority of the wavelet coefficients with values close to zero. A disadvantage with the discrete wavelet transform (DWT) is that it does not preserve translation invariance due to the subsampling performed. Therefore the stationary wavelet transform (SWT) [4], often referred to as the *a Trous Algorithm*, is usually applied. The SWT is a special version of the DWT, which uses upsampled versions of the filters in the filterbank between the scales in the tree, instead of decimating the coefficients at each scale. The cost of preserving the translation invariance is an overcomplete representation of the input signal. For images, the number of wavelet coefficients are three times the number of pixels in the input image *for each level* in the transform tree.

Examples of a speckle filter that perform MAP filtering on the wavelet coefficients of SWT filtered SAR images are found in [5, 6]. A LLMMSE filter operating on SWT transformed images is presented in [7]. The latter filter assumes that the image pixels are uncorrelated, and preforms despeckling by scaling each wavelet coefficient with the ratio of the variance of the noisy wavelet coefficient to the noise free one.

In this work we will also apply LLMMSE filtering of wavelet coefficients, but we assume that both the speckle free image and the speckle contribution are spatially correlated. We review a method for estimating the spectra of the radar cross section (RCS) and speckle from the single look complex (SLC) SAR image [8], and use these to derive the autocorrelations in the wavelet domain directly.

As most speckle filters, the filter proposed in this work assumes homogeneous areas. Thus, the SAR image is divided into blocks where the statistics can be considered to be homogeneous. However, we do not utilize sliding windows, which are popular for other methods. Instead, an adaptive quad-tree algorithm is applied to divide the SAR image into homogeneous regions. Unlike image-domain LLMMSE filters, filtering in the wavelet domain does not introduce boundary effects when filtering on non-sliding windows. This is because the wavelet coefficients are correlated, and each coefficient contains information on a neighborhood of pixels.

## 2. LMMSE FILTERING OF SPECKLE

In this section we review the linear minimum square error speckle filter.

The observed intensity $\mathbf{I}$ in a SAR image can be modeled as

$$\mathbf{I} = \sigma \mathbf{n}, \tag{1}$$

where the underlying RCS $\sigma$ and the speckle noise $\mathbf{n}$ are assumed to be statistically independent. Further, it is assumed that $\mathrm{E}\{\mathbf{n}\} = \mathbf{1}$, i.e. that the true RCS is the expected value of the observed intensity. The model in (1) is only a useful model if the autocorrelation $R_\sigma(\mathbf{r})$ is slowly varying compared to the system impulse response [8], i.e. for (locally) homogeneous areas.

As most methods for denoising signals generally are developed for additive noise, we have to express the speckle contribution as an additive term:

$$\mathbf{I} = \sigma + \sigma(\mathbf{n} - \mathbf{1}) = \sigma + \mathbf{v}, \tag{2}$$

where the speckle term $\mathbf{v}$ is *signal dependent*. This formulation enables the use of the linear property of the WT, which we will apply in section 4.

The minium mean square error (MMSE) estimate of $\boldsymbol{\sigma}$ is denoted as $\mathrm{E}\{\boldsymbol{\sigma}|\mathbf{I}\}$, which requires full knowledge of the statistical distributions of $\boldsymbol{\sigma}$ and $\mathbf{I}$. The linear MMSE (LMMSE) estimator is found by making a first order Taylor-Expansion of $\mathrm{E}\{\boldsymbol{\sigma}|\mathbf{I}\}$ around $\mathrm{E}\{\boldsymbol{\sigma}\}$, and is defined as [9]:

$$\hat{\boldsymbol{\sigma}} = \mathrm{E}\{\boldsymbol{\sigma}\} + \mathbf{C}_{\sigma I}\mathbf{C}_I^{-1}\left[\mathbf{I} - \mathrm{E}\{\mathbf{I}\}\right]\left(\mathbf{C}_{\sigma I}\mathbf{C}_I^{-1}\right)^T. \quad (3)$$

The multiplication with the rightmost factor $\left(\mathbf{C}_{\sigma I}\mathbf{C}_I^{-1}\right)^T$ is necessary since $\mathbf{I}$ is an image matrix, and we must apply the filter in both horizontal and vertical directions.

The cross-covariance matrix $\mathbf{C}_{\sigma I}$ can not be found directly, especially since we do not know $\boldsymbol{\sigma}$. By closer investigation, we find that

$$\mathbf{C}_{\sigma I} = \mathbf{R}_{\sigma I} - \mathrm{E}\{\boldsymbol{\sigma}\}\mathrm{E}\{\mathbf{I}\} = \mathbf{R}_\sigma - \bar{\boldsymbol{\sigma}}\bar{\boldsymbol{\sigma}}^T = \mathbf{C}_\sigma, \quad (4)$$

since the cross-correlation is expressed as

$$\mathbf{R}_{\sigma I} = \mathrm{E}\left\{\boldsymbol{\sigma}\mathbf{I}^T\right\} = \mathrm{E}\left\{\boldsymbol{\sigma}\left(\boldsymbol{\sigma}+\mathbf{v}\right)^T\right\} = \mathbf{R}_\sigma + \mathbf{R}_{\sigma v}, \quad (5)$$

$\mathbf{R}_{\sigma v} = \mathbf{0}$ due to statistical independence between $\boldsymbol{\sigma}$ and $\mathbf{n}$ and from the model (1) we have $\mathrm{E}\{\mathbf{n}\} = \mathbf{1}$.

By inserting (4) into (3), we express the LMMSE filter in the image domain as

$$\hat{\boldsymbol{\sigma}} = \bar{\boldsymbol{\sigma}} + \mathbf{C}_\sigma\mathbf{C}_I^{-1}\left[\mathbf{I} - \bar{\boldsymbol{\sigma}}\right]\left(\mathbf{C}_\sigma\mathbf{C}_I^{-1}\right)^T. \quad (6)$$

## 3. ESTIMATION OF COVARIANCE MATRICES

In this section we show how to estimate the autocorrelation matrices $\mathbf{C}_\sigma$ and $\mathbf{C}_I$ used in the filter equation (6).

Assuming that the statistics of the SAR image is at least wide sense stationary, the Wiener-Khinchin relation can be used to obtain the autocorrelation functions $R_I(\mathbf{r})$, $R_\sigma(\mathbf{r})$ and $R_n(\mathbf{r})$ from the autospectra $S_I(\mathbf{f})$, $S_\sigma(\mathbf{f})$ and $S_n(\mathbf{f})$, respectively.

in [8] Madsen has shown how to obtain the autospectra of the RCS and the speckle processes. Assuming a homogeneous SAR image, these can be computed as follows:

$$S_n(\mathbf{f}) = \delta(\mathbf{f})\left|\int |H(\xi)|^2\, d\xi\right|^2 + \int |H(\xi+\mathbf{f})|^2 |H(\xi)|^2\, d\xi, \quad (7)$$

where $|H(\mathbf{f})|^2 = S_{\mathbf{s}}(\mathbf{f})/\bar{\boldsymbol{\sigma}}$, and $\mathbf{s}$ is the complex observed SAR image, i.e. $\mathbf{I} = \mathbf{s}\circ\mathbf{s}^*$. Here $\circ$ denotes the Hermitian (element-wise) product.

$$S_\sigma(\mathbf{f}) = \frac{1}{T(\mathbf{0},\mathbf{0})}\left\{S_I(\mathbf{f}) - \frac{T'(\mathbf{f},\mathbf{0})}{2T(\mathbf{0},\mathbf{0})}\int S_I(\xi)\, d\xi\right\}, \quad (8)$$

where

$$T(\mathbf{r},\mathbf{f}) = \left|\int h(\mathbf{a})h^*(\mathbf{a}-\mathbf{r})\exp(-j2\pi\mathbf{f}\cdot\mathbf{a})\, d\mathbf{a}\right|^2, \quad (9)$$

and

$$T'(\mathbf{f},\mathbf{0}) = \int |H(\xi+\mathbf{f})|^2 |H(\xi)|^2\, d\xi. \quad (10)$$

The SAR system's impulse response is denoted by $h(\mathbf{r}) = \mathscr{F}^{-1}\{H(\mathbf{f})\}$, where $\mathscr{F}\{\cdot\}$ denotes the Fourier transform.

In practice, deriving $S_\sigma(\mathbf{f})$ from (8) is difficult since the integration has to be performed numerically and inaccuracies in estimating $S_I(\mathbf{f})$ are inevitable, especially if the estimation is based on small number of samples. We obtain better accuracy in the estimate of $R_\sigma(\mathbf{r})$ by considering

$$\mathbf{R}_I = \mathrm{E}\left\{\boldsymbol{\sigma}n(\boldsymbol{\sigma}n)^T\right\} = \mathrm{E}\left\{\boldsymbol{\sigma}\boldsymbol{\sigma}^T\right\}\mathrm{E}\left\{\mathbf{n}\mathbf{n}^T\right\} = \mathbf{R}_\sigma \circ \mathbf{R}_n. \quad (11)$$

Assuming homogeneous regions, we get

$$R_\sigma(\mathbf{r}) = \frac{R_I(\mathbf{r})}{R_n(\mathbf{r})}. \quad (12)$$

To achieve optimal accuracy in the estimation of the correlation matrices, we avoid numerical integration whenever possible. First, we observe that

$$S_n(\mathbf{f}) = \delta(\mathbf{f})T(\mathbf{0},\mathbf{0})(2\pi)^2 + T'(\mathbf{f},\mathbf{0}). \quad (13)$$

From (9) we have that

$$\begin{aligned} T(\mathbf{0},\mathbf{0}) &= \left|\int h(\mathbf{a})h^*(\mathbf{a})\, d\mathbf{a}\right|^2 = \left|\int |h(\mathbf{a})|^2\, d\mathbf{a}\right|^2 \\ &= \left|\frac{1}{(2\pi)^2}\int |H(\mathbf{f})|^2\, d\mathbf{f}\right|^2 \\ &= \left|\frac{1}{(2\pi)^2}\int \frac{1}{\bar{\boldsymbol{\sigma}}} S_s(\mathbf{f})\, d\mathbf{f}\right|^2. \end{aligned} \quad (14)$$

Applying the following property of a power density spectrum

$$\frac{1}{(2\pi)^2}\int S_s(\mathbf{f})\, d\mathbf{f} = \mathrm{A}\left\{\mathrm{E}\left\{|s(\mathbf{r})|^2\right\}\right\}, \quad (15)$$

and assuming that the process $s(\mathbf{r})$ is ergodic, we get

$$T(\mathbf{0},\mathbf{0}) = \left|\frac{1}{\bar{\boldsymbol{\sigma}}}\mathrm{E}\left\{|s|^2\right\}\right|^2 = 1. \quad (16)$$

Next, we recognize the integral in (10) as a convolution, which can be expressed with Fourier transforms as

$$\begin{aligned} T'(\mathbf{f},\mathbf{0}) &= |H(\mathbf{f})|^2 \star |H(\mathbf{f})|^2 \\ &= \mathscr{F}\left\{\left(\mathscr{F}^{-1}\left\{|H(\mathbf{f})|^2\right\}\right)^2\right\}. \end{aligned} \quad (17)$$

By inserting (17) and (16) into (13), $S_n(\mathbf{f})$ can be derived from $S_I(\mathbf{f})$ and $S_s(\mathbf{f})$, which both can be estimated from the SLC SAR image. Thus $S_n(\mathbf{f})$ can thus be estimated without numerical integrations.

We assume that the speckle and the terrain are isotropic, i.e. that the lag vector $\mathbf{r}$ in the autocorrelation function $R_n(\mathbf{r})$ can be replaced by the modulus,

$$R_n(\mathbf{r}) = R_n(|\mathbf{r}|) = R_n(r). \quad (18)$$

The same is true for $R_\sigma(\mathbf{r})$ and $R_I(\mathbf{r})$. This implies that the autocorrelation matrix $\mathbf{R}_I$ and therefor also the covariance matrix $\mathbf{C}_I$, will be a symmetric Toeplitz matrix, i.e.

$$\mathbf{R}_I = \begin{bmatrix} R_I[0] & R_I[1] & \cdots & R_I[N] \\ R_I[1] & R_I[0] & \cdots & R_I[N-1] \\ \vdots & \vdots & \ddots & \vdots \\ R_I[N] & R_I[N-1] & \cdots & R_I[0] \end{bmatrix}. \quad (19)$$

The same is true for $\mathbf{R}_\sigma$ and $\mathbf{C}_\sigma$.

We apply the averaged periodogram estimator to estimate the autospectra $S_I(f)$ and $S_n(f)$. As a consequence of the isotropic assumption (18), these spectra are also radially symmetric. Thus the averaged periodogram can be computed by estimating the spectrum in range direction and averaging in azimuth, or vice versa[1]. For a $N \times M$ sample of SAR data the spectrum $S_I(r)$ is estimated as

$$\hat{S}_I(f) = \frac{1}{M}\sum_{m=1}^{M}\left|\frac{1}{2\pi}\sum_{n=1}^{N} I(n,m)\exp(-j2fn/N)\right|^2. \quad (20)$$

To ensure that $R_I(r)$ and $R_\sigma(r)$ are valid autocorrelation functions, i.e. $R_\sigma(0) \geq R_\sigma(r), \forall r$, we apply an exponential model;

$$R_I(r) = ab^{-r} + c, \quad (21)$$

and similar for $R_\sigma(r)$. This is a common model in the image processing literature [10], and the exponential correlation function is often found to fit well to measured surfaces [11]. To estimate the parameters in (21), we use a nonlinear least-squares algorithm [12].

## 4. FILTERING IN WAVELET DOMAIN

In this section we develop the wavelet domain LMMSE speckle filter, equivalent to the image domain filter (6).

Because the WT is a linear transform, the wavelet coefficients of a SAR image can be viewed as

$$\mathbf{w}_I = \mathbf{w}_\sigma + \mathbf{w}_v, \quad (22)$$

where $\mathbf{w}_\sigma$ and $\mathbf{w}_v$ are the wavelet coefficients of the RCS and the additive, signal dependent speckle contribution, respectively. The LMMMSE filtering in the wavelet domain is performed in the same manner as in the image domain. Thus the wavelet domain analogy to (3) will be

$$\hat{\mathbf{w}}_\sigma = \mathrm{E}\{\mathbf{w}_\sigma\} + \mathbf{C}_{w_{\sigma I}}\mathbf{C}_{w_I}^{-1}\left[\mathbf{w}_I - \mathrm{E}\{\mathbf{w}_I\}\right]\left(\mathbf{C}_{w_{\sigma I}}\mathbf{C}_{w_I}^{-1}\right)^T. \quad (23)$$

Since the wavelet transform is a sparse transform, most wavelet-coefficients will have small values close to zero and $\mathrm{E}\{\mathbf{w}_\sigma\} = \mathrm{E}\{\mathbf{w}_I\} = \mathbf{0}$. This implies $\mathbf{C}_{w_\sigma} = \mathbf{R}_{w_\sigma}$ and $\mathbf{C}_{w_I} = \mathbf{R}_{w_I}$ Applying this in (23), the wavelet domain LMMSE filter becomes

$$\hat{\mathbf{w}}_\sigma = \mathbf{R}_{w_{\sigma I}}\mathbf{R}_{w_I}^{-1}\mathbf{w}_I\left(\mathbf{R}_{w_{\sigma I}}\mathbf{R}_{w_I}^{-1}\right)^T. \quad (24)$$

The autocorrelation matrices $\mathbf{R}_{w_\sigma}$ and $\mathbf{R}_{w_I}$ in the wavelet domain will be Toeplitz matrices like their image domain cousins, since the RCS and speckle processes are assumed to be wide sense stationary, and the WT is a linear transform. The one dimensional autocorrelation functions in the wavelet domain at scale $j$ will be given by

$$R_{w_I}^j(r) = R_{w_I}^{j-1}(r) * g_j^i(-r) * g_j^i(r), \quad i \in \{h,l\}, \quad (25)$$

where $g_j^h(r)$ and $g_j^l(r)$ are the highpass (wavelet) and lowpass (scaling) filters to obtain the detail and scaling coefficients at scale $j$, repsceticely. The transform is similar for $R_{w_\sigma}^j(r)$.

[1] A non-exhaustive test performed on Envisat ASAR and EMISAR data, showed no significant change in filtering performance when the direction of estimation was changed.

## 5. APPLYING THE FILTER LOCALLY

So far, we have considered the statistics of the SAR image to be homogeneous, which is generally not the case for real data. To remedy this, we apply the filter locally on blocks which can be considered to be homogeneous. The size of each block should be as large as possible, while still maintain homogeneity. The variance of the averaged periodogram estimator can be shown to be

$$\mathrm{var}\left\{\hat{S}_I(f)\right\} \simeq \frac{1}{M}S_I^2(f). \quad (26)$$

Thus, the accuracy of the estimated spectra will increase with increasing window size, and so does the performance of the filter.

We determine the window size by an adaptive method. First we start with a window of size $128 \times 128$ pixels. If the statistics in this window is found to be inhomogeneous, the window is divided in four parts and the procedure is repeated until homogeneity is achieved in all blocks. This is sometimes referred to as a quad-tree algorithm. We consider a window to be inhomogeneous if one of the following occurs:

i) The least squares algorithm [12] is unable to estimate the parameters in the exponential correlation model (21).
ii) The variance in the window is mores than twice of what we could expect in a homogeneous area, i.e. ENL $= \mathrm{E}\{I\}^2/\mathrm{var}\{I\} \leq 0.5$.

Figure 1 shows the resulting blocks structure for the input SAR image we have used in this paper.

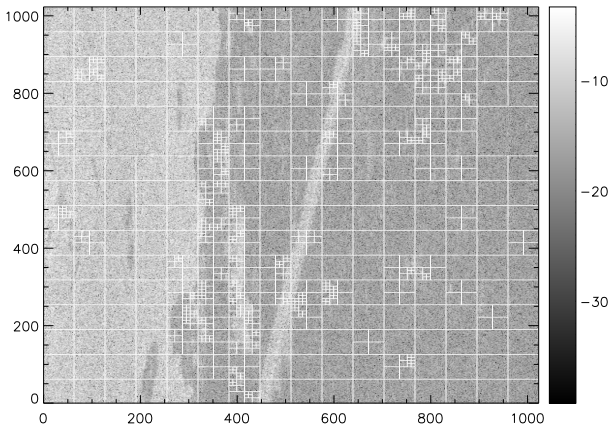


Figure 1: Input SAR image, displaying the local windows resulting from the quad-tree algorithm.

## 6. EXPERIMENTAL RESULTS

We compare the LLMMSE filtering in the wavelet domain (24) with the image domain equivalent (6) on a Envisat SAR image covering the area around the ESA calibration site in Flevoland. The test image is displayed in the top panels of Figure 2 and 3 in dB and amplitude, respectively.

In the wavelet domain filter, we utilize the SWT implemented in the Rice Wavelet Toolbox [13], with Daubechies $DB_2$ wavelet filters. The depth of the SWT is limited to four levels, as filtering on lower levels yields no significant

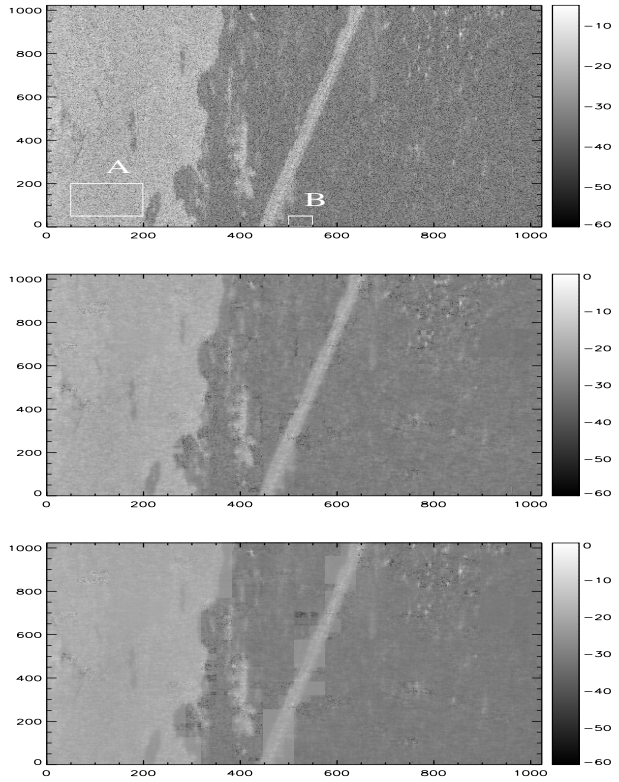


Figure 2: Original SAR image (top), filtered with proposed filter (middle) and filtered with LLMMSE filter in intensity domain (bottom). All images are displayed in dB.

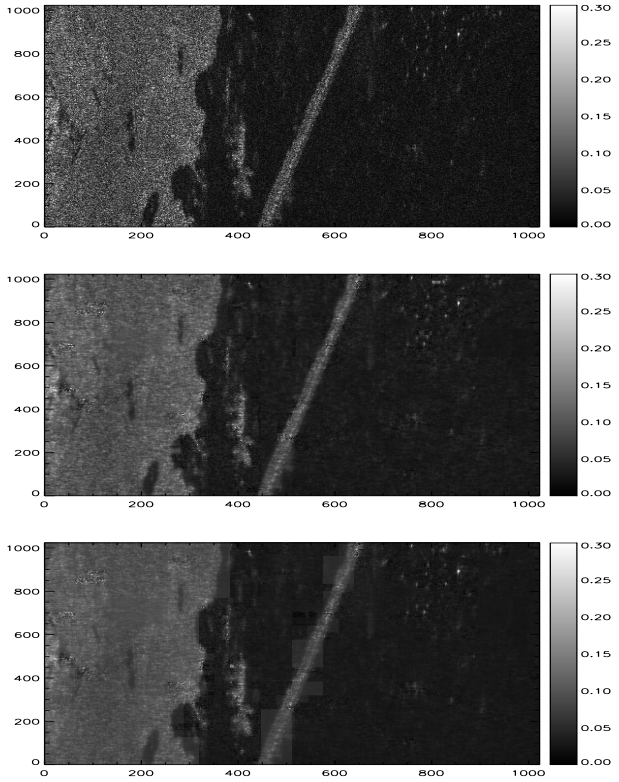

Figure 3: Original SAR image (top), filtered with proposed filter (middle) and filtered with LLMMSE filter in intensity domain (bottom). All images are displayed in amplitude

change in performance. Filtering is applied to all wavelet coefficients at the levels of the transform where the length of the wavelet filters $g_j^i(r)$ is less than the block size.

Investigating (23), we observe that the matrix multiplications actually means that we filter the wavelet coefficients by convolving each row and column of $\mathbf{w}_I$ by one column of $\mathbf{C}_{w_{\sigma I}}\mathbf{C}_{w_I}^{-1}$. To avoid introducing unnecessary artifacts on the boundary between the local blocks, we have to avoid to convolve these filters with zero data outside the edges of the blocks. We do this by using information from pixels in the neighboring blocks, where applicable.

We observe that both filters remove speckle, while preserving the point scatterers located in the upper left hand part of the image. From Figure 2 it seems that the image domain filter smooths more on the homogeneous areas over land, in the left hand part of the image. The image domain filter is also found to introduce more blurring than its wavelet domain cousin. Especially, we notice the boundary effects introduced by the image domain filter in the dike shown in the middle of the SAR image. These boundary effects are not introduced by the wavelet domain filter. The boundary effects is the reason why Kuan et al. suggested to use $12 \times 12$ overlapping windows for the image domain filter [2].

Figure 4 shows the estimated speckle contribution estimated from the two speckle filters, denoted as $\hat{\mathbf{n}} = \mathbf{I}/\hat{\boldsymbol{\sigma}}$. We observe that both speckle images represent looks like true speckle. In the areas surrounding strong scatterers in the SAR image, we observe that the speckle images are constant at 0dB, i.e. that no filtering has occurred. This is expected since dominant scatterers do not introduce speckle.

| Filter | Region A | | | Region B | | |
|---|---|---|---|---|---|---|
| | ENL | Bias | E$\{n\}$ | ENL | Bias | E$\{n\}$ |
| None | 0.97 | — | — | 0.99 | — | — |
| (24) | 10.8 | -9.07% | 0.97 | 12.9 | 8.9% | 0.84 |
| (6) | 20.9 | -17.2 % | 1.13 | 2.36 | 44% | 0.71 |

Table 1: Comparison between LLMMSE despeckling in the image and wavelet domain.

Some qualitative measurements on the performance of the two speckle filters are shown in Table 1, computed for the two regions A and B shown in Figure 2. Note that the image domain filter performs poorly in region B, due to the boundary effects. As observed, previously, Table 1 shows that the in the large homogeneous region A, the image domain filter has best smoothing. The wavelet domain filter introduces less bias than the image domain filter, and yields a speckle image with mean closer to the theoretical value $\mathrm{E}\{\mathbf{n}\} = \mathbf{1}$.

## 7. CONCLUSIONS AND FURTHER WORK

In this work we have developed a LLMMSE filter for SAR images operating in the wavelet domain. We have assumed that the speckle free image and the speckle contribution are spatially correlated. The correlation of both the RCS and speckle noise are estimated from the SLC images, which in turn are used to derive the autocorrelations in the wavelet

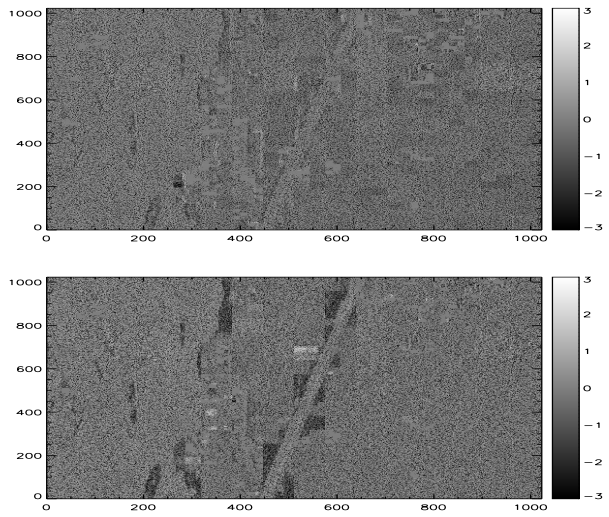

Figure 4: Resulting speckle images. Proposed filter (top) and intensity domain LLMMSE filter (bottom). The speckle images are displayed in dB.

domain.

We have proposed to apply the filtering on image blocks of unequal size, derived by a quad-tree algorithm. This increase computation time dramatically compared to sliding windows, which is common for image domain filters. Though, information from neighboring blocks are used to ensure convolution with valid data, but the percentage of overlap is small, especially for larger blocks. Applying the adaptive block-size strategy on image domain LLMMSE filtering still introduce some boundary effects, which are avoided by filtering in the wavelet domain.

Compare to its image domain equivalent, the wavelet domain LLMMSE filter introduces less bias, but yields less smoothing of homogeneous areas. To increase the smoothing of homogeneous areas further, a check on the level of homogeneity can be implemented and harder filtering performed for homogeneous ares, like for e.g. the Gamma-MAP filter [1].

In future work, the performance of the proposed filter will be tested more extensively against other speckle filters. Especially other wavelet based LLMMSE filters, like the one proposed in [7], to further explore the effect of taking into account the correlation of the wavelet coefficients.

## A. GENERATION OF INTENSITY IMAGES FROM SLC DATA

ASAR SLC data are typically oversampled to occupy around 80% of the bandwidth in range and azimuth. Squaring the magnitude directly will therefore introduce aliasing since $\mathbf{I} = \mathbf{s} \circ \mathbf{s}^*$ is equivalent to convolving $\mathbf{s}$ with itself in the frequency domain, which doubles the bandwidth of the signal. In this work we have oversampled the SLC data with 100% before processing. In this way we ensure no aliasing when generating the intensity images.

**Acknowledgment**

This work has been partly supported by the European Community, Environment and Sustainable Development Program under contract EVG1-CT-2002-00085 FloodMan. It has also been supported by the Norwegian Research Council under contract 153781/420.

## REFERENCES

[1] A. Lopès, E. Nezry, R. Touzi, and H. Laur, "Maximum a posteriori filtering and first order texture models in SAR images," in *proc. IGARSS '90*, Washington D.C., May 20–24 1990, pp. 2409–2412.

[2] D. T. Kuan, A. A. Sawchuck, T. C. Strand, and P. Chavel, "Adaptive restoration of images with speckle," *IEEE Transactions on Acoustics, Speech and Signal Processing*, vol. 35, no. 3, pp. 373–383, 1987.

[3] G. Strang and T. Nguyen, *Wavelets and filterbanks*, Wellesey-Cambridge Press, 1996.

[4] G. P. Nason and B. W. Silverman, "The stationary wavelet transform and some statistical applications," Tech. Rep. BS8 1Tw, University of Bristol, 1995.

[5] S. Foucher, G.B. Bénié, and J.-M. Boucher, "Multiscale MAP filtering of SAR images," *IEEE Transactions on image processing*, vol. 10, no. 1, pp. 49–60, Jan. 2001.

[6] S. Solbø and T. Eltoft, "Homomorphic wavelet-based statistical despeckling of SAR images," *IEEE Trans. Geosci. Remote Sensing*, vol. 42, no. 4, pp. 711–721, 2004.

[7] F. Argenti and L. Alparone, "Speckle removal from SAR images in the undecimated wavelet domain," *IEEE Transactions on Geoscience and Remote Sensing.*, vol. 40, no. 11, pp. 2363–2374, 2002.

[8] S. N. Madsen, "Spectral properties of homogeneous and nonhomogeneous radar images," *IEEE Trans. Aerospace and Elect. Systems*, vol. 23, no. 4, pp. 583–585, Jul. 1987.

[9] S. M. Kay, *Fudamentals of statistical signal processing, Volume I: Estimation theory*, Prentice Hall, 1993.

[10] R. C. Gonzalez and R. E. Woods, *Digital image processing*, Addison Wesley, 1992.

[11] J. A. Ogilvy, *Theory of Wave Scattering from Random Rough Surfaces*, Institute of Physics Publishing, 1991.

[12] D W Marquardt, "An algorithm for least-squares estimation of nonlinear parameters," *J. Soc. Indust. Appl. Math.*, vol. 11, pp. 431–441, 1963.

[13] R. Baraniuk et al., "Rice wavelet toolbox," http://www-dsp.rice.edu/software/rwt.shtml, Digital Signal Processing Group, Rice University, 2001.